Ultrasonics 93 (2019) 145–155

Contents lists available at ScienceDirect

Ultrasonics

journal homepage: www.elsevier.com/locate/ultras

Damage prediction via nonlinear ultrasound: A micro-mechanical approach

J. Melchor[a,b,c,*], W.J. Parnell[d], N. Bochud[e], L. Peralta[f], G. Rus[a,b,c]

[a] Department of Structural Mechanics, University of Granada, Granada, Spain
[b] IBS Biosanitary Research Institute, Granada, Spain
[c] MNat Scientific Unit of Excellence, University of Granada, Spain
[d] School of Mathematics, University of Manchester, Oxford Road, Manchester M13 9PL, UK
[e] Institut Langevin, ESPCI Paris, CNRS (UMR 7587), PSL Research University, 75005 Paris, France
[f] Biomedical Engineering Department, School of Biomedical Engineering and Imaging Sciences, King's College London, London, UK

ARTICLE INFO

Keywords:
Non-destructive evaluation
Nonlinear elasticity
Ultrasound
Homogenization
Micro-cracks
Nonlinear acoustics

ABSTRACT

Nonlinear constitutive mechanical parameters, predominantly governed by micro-damage, interact with ultrasound to generate harmonics that are not present in the excitation. In principle, this phenomenon therefore permits early stage damage identification if these higher harmonics can be measured. To understand the underlying mechanism of harmonic generation, a nonlinear micro-mechanical approach is proposed here, that relates a distribution of clapping micro-cracks to the measurable macroscopic acoustic nonlinearity by representing the crack as an effective inclusion with Landau type nonlinearity at small strain. The clapping mechanism inside each micro-crack is represented by a Taylor expansion of the stress-strain constitutive law, whereby nonlinear terms arise. The micro-cracks are considered distributed in a macroscopic medium and the effective nonlinearity parameter associated with compression is determined via a nonlinear Mori-Tanaka homogenization theory. Relationships are thus obtained between the measurable acoustic nonlinearity and the Landau-type nonlinearity. The framework developed therefore yields links with nonlinear ultrasound, where the dependency of measurable acoustic nonlinearity is, under certain hypotheses, formally related to the density of micro-cracks and the bulk material properties.

1. Introduction

Conventional ultrasonic non-destructive evaluation (NDE) methods are sensitive to gross defects, but are generally much less sensitive to distributed micro-cracks [1–4]. Furthermore, general degradation of strength is often found in apparently flawless materials [5]. It is well known that material failure is usually preceded by some aspect of nonlinear mechanical behaviour before significant plastic deformation or material damage occurs [6]. It is acknowledged that the level of material degradation can be evaluated by measuring some aspect of acoustic nonlinearity. In particular for example one would expect that damage would affect the magnitude of higher-order harmonics, the presence of which is solely due to nonlinear effects. The relation between damage level and acoustic nonlinearity has been observed and demonstrated extensively in many configurations. The so-called *finite-amplitude technique* [7] has been proven to be useful for non-destructive detection of defects in ceramics [8], concrete structures [9,10], composites [11], as well as fatigue cracks in metals, such as steels, titanium, and aluminum alloys [12,13].

The induced nonlinearity, present at small strains, is attributed to e.g. Hertzian contact and other micro-structural effects such as internal stresses, micro-cracks, zero-volume disbonds, and usually precedes the main cracking mechanisms and the subsequent failure of the material. A common way of viewing these defects is to consider that the nonlinear acoustic response is due to an internal interface that separates the intact material and the inclusion. This contact interface can be either free (large pores, opened cracks), partially clamped ("clapping" mechanism between the opened/closed crack states), or ideally bonded, and is thought to be mostly responsible for the large ultrasonic nonlinear response of degraded materials [14]. Considerable experimental work has shown that cracks and imperfect interfaces can behave in a nonlinear fashion [15,16] and have thus opened up new opportunities to detect partially closed cracks that would be much more difficult to identify with conventional linear methods.

Theoretically, acoustic nonlinearity manifests itself in higher order strain contributions to a macroscopic strain energy function (SEF) associated with the material, thus giving rise to nonlinear stress-strain relationships and effective nonlinear elastic moduli [17]. Of specific

* Corresponding author at: Department of Structural Mechanics, University of Granada, 18071 Granada, Spain.
E-mail address: jmelchor@ugr.es (J. Melchor).

https://doi.org/10.1016/j.ultras.2018.10.009
Received 9 April 2018; Received in revised form 2 October 2018; Accepted 20 October 2018
Available online 28 October 2018

interest is how these moduli depend on the micro-structure. In particular in the bone community, where the interest is on the dependence of these parameters on the presence of damage, usually assumed to be micro-cracks, Renaud et al. [4] state "*However, little work has been done on the relationship between crack density and level of elastic nonlinearity*" and in Muller et al. [3] "*From empirical evidence it is clear that micro-cracks are responsible for the enhanced nonlinear response…we have no quantitative link between damage quantity and nonlinear response.*" It therefore appears to be of importance to build theoretical models that can attempt to provide these links [18–20].

The problem of determining the effective *linear* elastic properties of an inhomogeneous material has been studied extensively [21–23]. A popular approach in micro-mechanics is to characterize the heterogeneous medium via dispersions of inclusions or inhomogeneities [24] and a plethora of approximations have been proposed in order to approximate effective properties based on a spheroidal or ellipsoidal inclusion approximation thanks to the classical results of Eshelby [25,26]. Eshelby's tensor also arises in convenient bounds on linear elastic properties of inhomogeneous media [27,28].

Extensions of these schemes to accommodate the case of cracked media in the linear (static) regime when the cracks are assumed open (traction free), have been carried out in numerous studies, see e.g. [29–31]. However, often overlooked is the effective low frequency *dynamic* response where cracks can be in either opened or closed states (or more complex loadings) depending upon whether, for example, the crack is in a compressive or tensile cycle of the propagating wave. Furthermore, the effect of *nonlinear* crack response can be significant.

The extension of the homogenization procedure in order to incorporate nonlinear inhomogeneities, based on Eshelby's theory, was developed by Giordano et al. [32], who obtained the bulk and shear moduli along with the nonlinear Landau coefficients of the overall material in terms of the elastic behaviour of the constituents and of their volume fractions, all in the context of small strain. Two types of nonlinear inclusions were investigated, spherical and parallel cylindrical inclusions, both of which were embedded into a linear homogeneous and isotropic matrix. In this context the material is considered to behave in a constitutively nonlinear manner under small strains (i.e. it is geometrically linear) [25,32,33,26].

In this work, a micro-mechanical model is proposed to relate the density of nonlinear micro-cracks to the macroscopic acoustic nonlinearity. To this end, the damaged material is idealized as a composite material: initially a dispersion of *nonlinear* isotropic spheroidal inclusions surrounded by a linear isotropic matrix. At the micro-scale, the clapping mechanism excited inside each micro-crack during ultrasonification is approximated by a Taylor expansion of the bilinear stress-strain constitutive law and the expansion is truncated at the quadratic term. This approximation is linked to the acoustic nonlinearity by rearranging the nonlinear Landau constitutive law. This approximation is convenient from an analytical viewpoint and permits progress to be made in terms of potential interpretation of micro-structural modelling of damaged materials. It is, of course, important to note that there are multiple other possible sources of nonlinearity that we do not treat here. This includes hysteretic clapping, the crack tip plastic zone, partial closure and atomistic nonlinearities. [34–39].

Returning to the quadratic nonlinearity considered here as an approximation to nonlinear clapping, Eshelby's tensor is employed within the Mori-Tanaka homogenization process [40], where the clapping micro-cracks are represented by *effective* nonlinear penny-shaped inclusions. The penny-shaped cracks are assumed to be aligned, as a consequence of a preferential fatigue load direction of the structure. The nonlinearity of the inclusions can therefore be described by the so-called Landau coefficients, which measure the deviation from linearity. Finally, the relationships between these Landau coefficients and the measurable acoustic nonlinearity in ultrasound are presented.

It should be stressed that micro-mechanics can be employed in the context of linear and nonlinear acoustics described here because we are well into the so-called *separation of scales regime*, where propagating wavelengths are much larger than the defect or crack under consideration. Their response is thus quasi-static. For simplicity in this model we also neglect the nonlinear response in shear.

The article proceeds as follows. In Section 2 we introduce the framework of micro-mechanics and upscaling employed in order to determine the effective parameters associated with a cracked medium, beginning with the simple linear response of a cracked medium where penny-shaped cracks are modelled as traction free and ending with derivations of the effective nonlinear acoustic parameter associated with a damaged medium. A nonlinear clapping model associated with a single crack is introduced in Section 3 and parameters associated with this model are then linked to an effective nonlinear inclusion model of the nonlinear crack response. These parameters are then fed into the general framework of effective acoustic nonlinearity in Section 4 where effective properties are derived in terms of the third order elastic constant C (associated with compressional nonlinearity), anisotropy coefficients and the density of microcracks. Finally, Section 5 explores a specific configuration where the model can be employed to predict the effective nonlinear parameter associated with a damaged bone sample, although it should be stated that the methodology is potentially useful for a broad range of damaged media. We close with discussion in Section 6.

2. Micro-mechanics framework

We model a damaged material in a similar manner to a composite material, as in e.g. [41–43]. In particular we are interested in the effect that damage, or more specifically micro-cracks, have on the effective mechanical properties of the medium and how this subsequently affects the *nonlinear* acoustic response of the material. We model these cracks as the limit of aligned spheroidal cavities as we shall explain shortly.

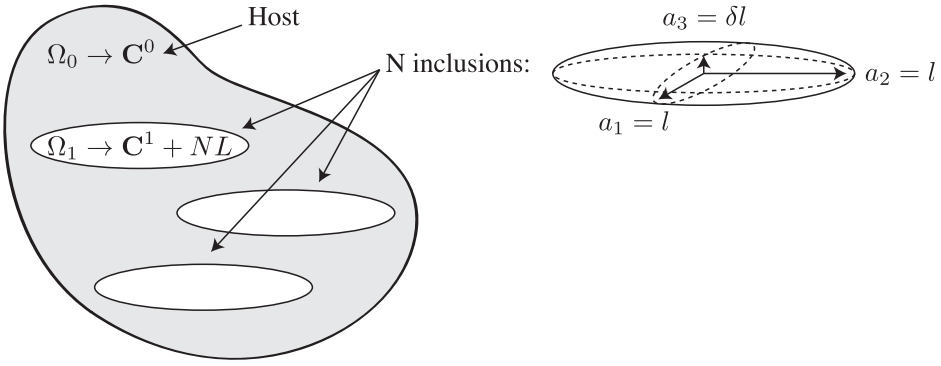

Fig. 1. Outline of the considered medium: dispersion of nonlinear spheroidal inclusions in a linear isotropic host with distribution of microcracks defined by density $\alpha = \phi/\delta$ where ϕ is the volume fraction.

Furthermore we shall consider these cracks to behave nonlinearly.

Start by considering the case as depicted in Fig. 1 when a medium Ω has within it two elastic phases Ω_0 (the *linear elastic* host or matrix with elastic modulus tensor $\mathbf{C}^0$ and compliance tensor $\mathbf{D}^0$ such that $\mathbf{C}^0\mathbf{D}^0 = \mathbf{I}$ where $\mathbf{I}$ is the fourth order identity tensor) and a collection of N inclusions that comprise the phase Ω_1. We do not restrict the elastic behaviour of the inclusion phase to be linear. We suppose that the inclusions are aligned spheroids with semi-axes $a_1 = a_2 = \ell$ and a_3 in the x_1, x_2 and x_3 directions respectively, defining the aspect ratio $\delta = a_3/\ell$ so that $\delta < 1$ ($\delta > 1$) for oblate (prolate) spheroids.

Referring to Fig. 1, the volume of cracks vanishes in the strongly oblate limit of spheroidal cavities, i.e. $\delta \to 0$ and so the effective contribution of the vanishing inclusion volume fraction has to be defined in this limit. The volume fraction ϕ of the inclusion phase is defined by

$$\phi = \frac{|\Omega_1|}{|\Omega|} \tag{1}$$

where $|\Omega|$ denotes the volume of the domain Ω. The volume fraction ϕ clearly tends to zero in the limit $\delta \to 0$. This motivates the introduction of the *density* of microcracks

$$\alpha = \frac{\phi}{\delta} = \frac{N(4\pi/3)\ell^3}{|\Omega|} \tag{2}$$

which is finite as $\delta \to 0$, and can also be interpreted as the volume fraction of the spherical inclusions that would have the same footprint or projection as the flat penny-shaped inclusions (of zero volume). Alternatively, if the penny-shaped inclusions were inflated to make them spherical, their volume fraction would be α.

We employ the Mori-Tanaka method [40] in order to determine the effective behaviour of the medium, describing in succession first a brief summary of the linear elastic case and more importantly in detail the extension to incorporate nonlinear (clapping) effects. Let $\mathbf{T}$ be the Cauchy stress and $\mathbf{E}$ the linear strain. The average stress within the medium is straightforwardly determined as [32]

$$\bar{\mathbf{T}} = \mathbf{C}^0\bar{\mathbf{E}} - \phi\mathbf{C}^0\bar{\mathbf{E}}^1 + \phi\bar{\mathbf{T}}^1\{\bar{\mathbf{E}}^1\} \tag{3}$$

where the curly parentheses in $f\{\cdot\}$ denote an argument of the function f and where $\overline{f}^r$ denotes the volume average over the rth phase, i.e.

$$\overline{f}^r = \frac{1}{|\Omega_r|}\int_{\Omega_r} f\{\mathbf{x}\}d\Omega_r. \tag{4}$$

Note that the general form for $\bar{\mathbf{T}}^1\{\bar{\mathbf{E}}^1\}$ is retained since we have not yet specified the constitutive behaviour of the inclusion.

2.1. Micro-mechanics for linear elastic particulate media

To employ the Mori-Tanaka method for the linear case, first assume that the inclusion is linear elastic, so that $\bar{\mathbf{T}}^1 = \mathbf{C}^1\bar{\mathbf{E}}^1$ and for an isolated inclusion Eshelby's result is

$$\mathbf{E}^\infty = \bar{\mathbf{E}}^0 = (\mathbf{I} + \mathbf{S}(\mathbf{D}^0\mathbf{C}^1 - \mathbf{I}))\bar{\mathbf{E}}^1 \tag{5}$$

where $\mathbf{E}^\infty$ denotes the (uniform) strain in the far field and $\mathbf{S}$ is the (uniform) Eshelby tensor. Determining the volume average of the strain $\bar{\mathbf{E}}$ in terms of $\bar{\mathbf{E}}^1$ then yields $\bar{\mathbf{T}} = \mathbf{C}^*\bar{\mathbf{E}}$, where

$$\mathbf{C}^* = \mathbf{C}^0 + \phi(\mathbf{C}^1 - \mathbf{C}^0)[\phi\mathbf{I} + (1-\phi)(\mathbf{I} + \mathbf{S}(\mathbf{D}^0\mathbf{C}^1 - \mathbf{I}))]^{-1}. \tag{6}$$

The above approach summarizes the Mori-Tanaka method. Even though we have assumed a dilute dispersion of ellipsoids, the result (6) is *feasible* for non-dilute volume fractions in that it recovers the limit $\mathbf{C}^* \to \mathbf{C}^1$ as $\phi \to 1$.

2.2. Linear elasticity: open cracks in a homogeneous matrix

Consider now the strongly oblate limit of the spheroidal cavity, i.e. $\delta \to 0$ and $\phi \to 0$ together with $\mathbf{C}^1 = \mathbf{0}$. The latter means that Eshelby's result becomes

$$\mathbf{E}^1 = (\mathbf{I} - \mathbf{S})^{-1}\mathbf{E}^0 = \mathbf{F}\mathbf{E}^0. \tag{7}$$

which is interpreted as an induced strain. Since $\mathbf{E}^0 = O(1)$ and the tensor $\mathbf{F}$ defined via $\mathbf{F} = (\mathbf{I} - \mathbf{S})^{-1} = O(1/\delta)$ (see Appendix A), we have $\mathbf{E}^1 = O(1/\delta)$. Using this in the average strain expression $\bar{\mathbf{E}} = (1-\phi)\bar{\mathbf{E}}^0 + \phi\bar{\mathbf{E}}^1$, together with (3) when $\bar{\mathbf{T}}^1 = \mathbf{0}$ yields $\bar{\mathbf{T}}^* = \mathbf{C}^*\bar{\mathbf{E}}$ where

$$\mathbf{C}^* = \mathbf{C}^0 - \phi\mathbf{C}^0\mathbf{F}[(1-\phi)\mathbf{I} + \phi\mathbf{F}]^{-1}. \tag{8}$$

Employing (2) means that (8) becomes

$$\mathbf{C}^* = \mathbf{C}^0 - \alpha\mathbf{C}^0\mathbf{G}[(1-\delta\alpha)\mathbf{I} + \alpha\mathbf{G}]^{-1}, \tag{9}$$

where we have defined $\mathbf{G} = \delta\mathbf{F}$. Now take the limit $\delta \to 0$ and introduce

$$\mathcal{G} = \lim_{\delta\to 0}\mathbf{G} = \lim_{\delta\to 0}\Big(\delta\mathbf{F}\Big) = O(1). \tag{10}$$

The non-zero components of the transversely isotropic tensor $\mathcal{G}$ are listed in (A.22) of Appendix A. Results are now obtained in terms of the modified volume fraction α, noting that $\mathcal{G}$ is independent of α. The expression for $\mathbf{C}^*$ therefore becomes, in the penny-shaped crack limit [32]

$$\mathbf{C}^* = \mathbf{C}^0(\mathbf{I} - \alpha\mathcal{G}[\mathbf{I} + \alpha\mathcal{G}]^{-1}). \tag{11}$$

It should be noted that the above analysis requires only the input from the influence of a single crack feature, defined by its Eshelby tensor limit. A comparison of such methods with numerical methods associated with asymptotic homogenization in the antiplane elastic case, where cracks are arranged on a periodic lattice, was provided in [44].

We wish to understand how the above is extended to the case of nonlinear inclusions. We will do this shortly, but first as a precursor to this problem, let us consider how one can incorporate more complicated (linear) crack face traction effects.

2.3. Linear elasticity: allowing for crack face effects

The mechanism for incorporating the effects of the crack face shall now be considered by scaling the inhomogeneity properties $\mathbf{C}^1$ on δ instead of taking it to be identically zero in the case of open cracks. Let us assume that as $\delta \to 0$, $\mathbf{T}^1 = \mathbf{C}^1\mathbf{E}^1 \sim \delta\widetilde{\mathbf{C}}^1\mathbf{E}^1$ where $\widetilde{\mathbf{C}}^1 = O(1)$. Using this in Eshelby's result (5) we find that

$$\mathbf{E}^0 = (\mathbf{I} - \mathbf{S} + \delta\mathbf{H})\mathbf{E}^1 \tag{12}$$

$$= (\mathbf{I} - \mathbf{S})(\mathbf{I} + \delta(\mathbf{I} - \mathbf{S})^{-1}\mathbf{H})\mathbf{E}^1 \tag{13}$$

where we have written $\mathbf{H} = \mathbf{S}\mathbf{D}^0\widetilde{\mathbf{C}}^1$, which we note is $O(1)$ as $\delta \to 0$. Given that $\mathbf{F} = (\mathbf{I} - \mathbf{S})^{-1} = O(1/\delta)$ the term involving $\mathbf{H}$ now contributes an "extra stress" associated with crack face effects. Once again using the average strain expression we find that

$$\mathbf{E}^1 = \mathbf{F}[(1-\alpha\delta)(\mathbf{I} + \mathbf{H}\delta\mathbf{F}) + \alpha\delta\mathbf{F}]^{-1}\bar{\mathbf{E}} \tag{14}$$

and the averaged stress is

$$\bar{\mathbf{T}} = \mathbf{C}^0\bar{\mathbf{E}} - \alpha\mathbf{C}^0\delta\mathbf{E}^1 + \alpha\widetilde{\mathbf{C}}^1\delta^2\mathbf{E}^1. \tag{15}$$

Note that the coefficient of the last term here is $O(\delta^2)$ so that in the limit, this term will tend to zero since $\mathbf{E}^1 \sim O(1/\delta)$. The "extra stress" therefore arises purely due to the Eshelby result and not due to averaged stress.

Therefore, using (14) in (15) and taking the penny-shaped crack limit $\delta \to 0$, we obtain

$$\bar{\mathbf{T}} = \mathbf{C}^0(\mathbf{I} - \alpha\mathcal{G}[\mathbf{I} + \mathbf{H}\mathcal{G} + \alpha\mathcal{G}]^{-1})\bar{\mathbf{E}} \tag{16}$$

noting that if we take $\widetilde{\mathbf{C}}^1 \to 0$ (so that $\mathbf{H} = 0$) we recover (11). As should be expected, the effect of a non-zero $\mathbf{H}$ has the effect of stiffening the material. In particular for example, in dynamics where a compressive wave will give rise to both open cracks (in tension) and closed cracks

(in compression) the effective Young's modulus cannot be that due to the open crack case considered above. Expression (16) is the correction to that result.

2.4. Micro-mechanics for nonlinear cracks

Let us now assume that the stress-strain condition for the inclusion is *nonlinear*, taking the form $\mathbf{T}^1 = \mathbf{T}^1_L + \mathbf{T}^1_{NL}$ associated with linear and nonlinear effects respectively, with the intention of modelling the behaviour of cracks. The form of the nonlinear term will be discussed shortly but since in general its leading form will be quadratic in the strain, we shall see that it needs an additional δ scaling in order to have an $O(1)$ effect and remain bounded, i.e. this requires $\mathbf{T}^1_{NL} = \delta^2\widetilde{\mathbf{T}}^1_{NL}$, where $\widetilde{\mathbf{T}}^1_{NL} \sim (\mathbf{E}^1)^2$ so that scaling the linear term as in the previous section to accommodate linear crack face effects,

$$\mathbf{T}^1 = \delta\widetilde{\mathbf{C}}^1\mathbf{E}^1 + \delta^2\widetilde{\mathbf{T}}^1_{NL}. \tag{17}$$

Later on in Section 3 we justify this scaling from a study of the local crack problem. It has been shown that for constitutive nonlinearity in the strain, the Eshelby result for spheroids holds and gives (with appropriate modifications to scalings as considered here) [32]

$$\mathbf{E}^0 = ((\mathbf{I} - \mathbf{S}) + \delta\mathbf{H})\mathbf{E}^1 + \delta^2\mathbf{S}\mathbf{D}^0\widetilde{\mathbf{T}}^1_{NL}. \tag{18}$$

Using this in the average strain yields, after some work (and recalling that curly parentheses denote the argument of the function)

$$\bar{\mathbf{E}} = (\mathbf{I} + \mathbf{H}\mathbf{G} + \alpha\mathbf{G})\mathbf{F}^{-1}\mathbf{E}^1 + \mathbf{S}\mathbf{D}^0\widetilde{\mathbf{T}}^1_{NL}\{\delta\mathbf{E}^1\} + O(\delta) \tag{19}$$

where we have retained only terms that will become important in the penny shaped limit and we note that we have conveniently put the δ inside the argument of the nonlinear stress term which is quadratic in its argument. Now we have to *formally invert* this expression which gives,

$$\mathbf{E}^1 = \mathbf{F}[\mathbf{I} + \mathbf{H}\mathbf{G} + \alpha\mathbf{G}]^{-1}\bar{\mathbf{E}} - \mathbf{F}\mathbf{U}\{\bar{\mathbf{E}}\} \tag{20}$$

where $\mathbf{U}\{\bar{\mathbf{E}}\}$ refers to the first, quadratic nonlinear contribution to this equation, which it transpires, takes the form

$$\mathbf{U}\{\bar{\mathbf{E}}\} = (\mathbf{I} + \mathbf{H}\mathbf{G} + \alpha\mathbf{G})^{-1}\mathbf{S}\mathbf{D}^0\widetilde{\mathbf{T}}^1_{NL}\{\mathbf{G}(\mathbf{I} + \mathbf{H}\mathbf{G} + \alpha\mathbf{G})^{-1}\bar{\mathbf{E}}\}. \tag{21}$$

Finally, using (20) in the average stress Eq. (3) and taking the penny-shaped crack limit, we find

$$\bar{\mathbf{T}} = \mathbf{C}^0(\mathbf{I} - \alpha\mathcal{G}[(\mathbf{I} + \mathbf{H}\mathcal{G}) + \alpha\mathcal{G}]^{-1})\bar{\mathbf{E}} - \mathbf{C}^0\alpha\mathcal{G}\mathcal{U}\{\bar{\mathbf{E}}\} \tag{22}$$

where

$$\mathcal{U}\{\bar{\mathbf{E}}\} = (\mathbf{I} + \mathbf{H}\mathcal{G} + \alpha\mathcal{G})^{-1}\mathbf{S}\mathbf{D}^0\widetilde{\mathbf{T}}^1_{NL}\{\mathcal{G}(\mathbf{I} + \mathbf{H}\mathcal{G} + \alpha\mathcal{G})^{-1}\bar{\mathbf{E}}\}. \tag{23}$$

Note once again that if we take the limit when nonlinear effects are negligible, $\mathcal{U} \to 0$, we recover the linear limit of the previous section and the result (16).

Eq. (22) is therefore the extension of the homogenization procedure to the nonlinear (small strain) setting for penny shaped cracks. We now restrict the form of nonlinearity in order to identify a specific nonlinear constitutive parameter that can be used to identify damage via nonlinear ultrasonic testing.

3. Nonlinear crack clapping model

In this section we describe the formulation of the nonlinear constitutive model of an individual micro-crack, which is later equated to an effective nonlinear inclusion for use in the micro-mechanical method described above. As opposed to linear crack analysis, which the literature treats as open (since closed cracks transmit compressional forces as if the material were intact), the nonlinear behaviour of cracks correctly models a range of states, either closed (for negative strains) or open (for positive strains). The clapping contact mechanism associated with a cyclic load exerted by oscillatory movement of the nonlinear ultrasonification behaves as follows: while the cracks tend to be closed at rest, once subject to the cyclic stress, cracks close during the compressional half-cycle, transmitting stress and establishing displacement continuity, whereas during crack opening under tension, the stress inside the crack vanishes and a displacement discontinuity arises across the crack face.

3.1. Nonlinear formulation

This local clapping contact phenomenon gives rise to a nonlinear stress-strain relation at the defect [45]. Pecorari et al. [46] proposed a 1D clapping model for extension in the x_3 direction, where the crack face is in the x_1x_2 plane (referring to Fig. 1) with different elastic moduli for compression and tension, i.e.

$$T^c_{33} = \mathcal{E}_0\left(1 - H\{E^c_{33}\}\left(\frac{\Delta\mathcal{E}}{\mathcal{E}_0}\right)\right)E^c_{33} \tag{24}$$

where the superscript c here refers to the fact that this is intended to be the constitutive response of the crack. Later we will equate this to an effective nonlinear inclusion (with superscripts 1), thus relating the crack properties to an effective inclusion. Furthermore here, $H\{E_{33}\}$ is the Heaviside step function, $\mathcal{E}_0$ is the *host* Young's modulus under compression, and $\Delta\mathcal{E}$ is its change under stress reversal to tension. We assume that the elastic modulus under tension is negligible and therefore $\Delta\mathcal{E} = \mathcal{E}_0$. In fact this will be non-zero in reality and below we argue that for nonlinear effects to become important it should scale as δ^2. The further assumption is that all other components of stress act linearly in the strain components.

It transpires to be more simple to treat only volumetric components of stress and strain we shall describe in the next subsection, thus permitting us to obtain a one-dimensional compressional constitutive law that relates crack pressure $p^c = -\frac{1}{3}\mathrm{tr}\mathbf{T}^c$ to crack volumetric strain $v^c = -\frac{1}{3}\mathrm{tr}\mathbf{E}^c$ (where $\mathbf{E}^c$ is the induced crack strain) capturing the compressive or opening states of the crack behaviour in a single direction, and so we write

$$p^c = 3K\{v^c\}v^c \tag{25}$$

where $K\{v^c\}$ is the strain dependent bulk modulus. Hence, from Eq. (24), the bilinear stiffness of the proposed model with multiple microcracks is proposed in the form

$$K\{v^c\} = K_0(1 - H\{v^c\}) \tag{26}$$

where $K_0 = \lambda_0 + 2\mu_0/3$ is the linear elastic bulk modulus of the host material.

In order to bypass the difficulty of engaging with a non-differentiable function for the stress-strain law (via the extraction of a Taylor expansion of the Heaviside function) we approximate (26) by a logistic function with *sharpness parameter* $\mathcal{N}$:

$$K\{v^c\} \simeq K_0\left(1 - \frac{1}{1 + e^{-\delta^2\mathcal{N}v^c}}\right). \tag{27}$$

When homogenizing, note that the assumption of common alignment of cracks is made, as well as negligible residual stresses that would be responsible for differences in the strain where the "kink" appears at the origin. These are averaged out via the smoothed bilinear form. The bilinear stiffness is now approximated by a Taylor expansion of (27) for small δ, i.e.

$$K\{v^c\} \simeq K_0\left(\frac{1}{2} - \frac{\delta^2\mathcal{N}v^c}{4} + O((v^c)^2)\right). \tag{28}$$

The parameter $\mathcal{N}$ is a parameter that conveys nonlinearity, in this case it is associated with the crack under tension and is required to be measured via experiment. The scaling δ^2 is such that the nonlinear term can contribute to the homogenized properties as described in Section 2.4. One could also consider an $O(\delta)$ term if one wished (adding such a

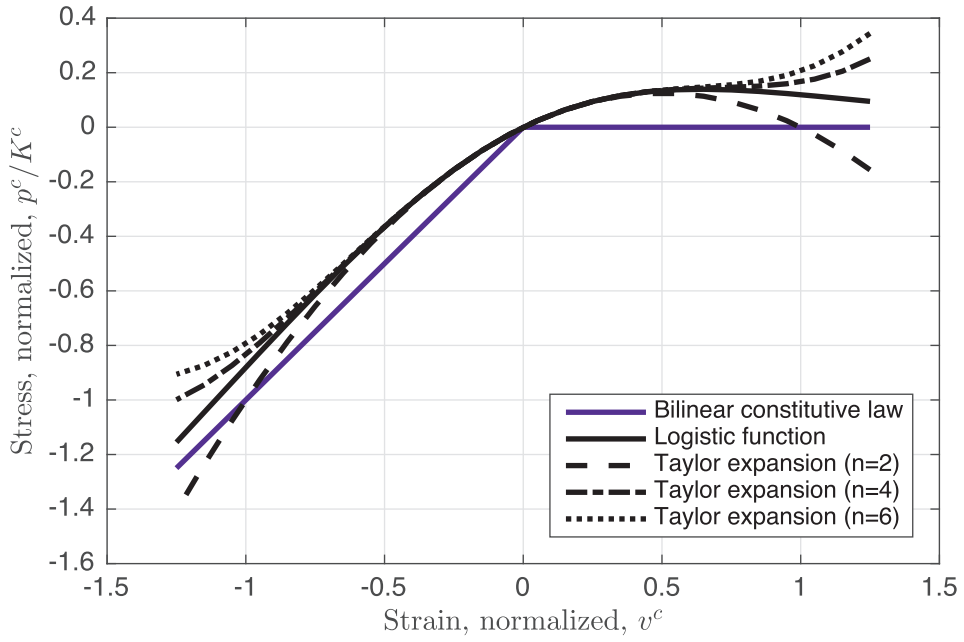

Fig. 2. Illustration of the exact bilinear constitutive law, its approximation via the logistic function and associated Taylor expansions, employing the fitting parameter combination $\delta^2\mathcal{N} = 7.2 \times 10^4$.

term in the exponent of the exponential function in (27)) in order to take into account *linear* crack face effects, as discussed in Section 2.3 but here our interest resides in nonlinear effects only. In Fig. 2 we plot the different approximations to the bilinear response, taking $\delta^2\mathcal{N} = 7.2 \times 10^4$, a value which is discussed further in Section 5.

The result (28) essentially says that the first linear approximation contains half open (zero modulus) and half closed cracks (intact modulus). This average yields an effective bulk modulus of the inclusion of $K_0/2$, which coincides with the first linear tangent term of the Taylor expansion.

We now write the crack response in tensor form. Since any second order isotropic tensor (stress or strain) can be split into volumetric (scalar) and deviatoric (tensor) parts, the constitutive equation can be rearranged as particular cases of the following general form

$$\mathbf{T}^c = \underbrace{-p^c\mathbf{I}_2}_{\text{volumetric}} + \underbrace{\mathbf{T}^c_D}_{\text{deviatoric}}, \quad p^c = -\frac{1}{3}\text{tr}\mathbf{T}^c. \tag{29}$$

where $\mathbf{I}_2$ is the *second* order identity tensor with components $(\mathbf{I}_2)_{ij} = \delta_{ij}$. The strain is also decomposed similarly,

$$\mathbf{E}^c = -v^c\mathbf{I}_2 + \mathbf{D}^c, \quad v^c = -\frac{1}{3}\text{tr}\mathbf{E}^c. \tag{30}$$

The linear elastic dependency is enriched with quadratic terms, following the series expansion concept put forth by Landau [47]. Only the volumetric part is detailed in terms of a nonlinearity parameter β due to the scalar nature of the volumetric strain v. Further since experimentally only compressional ultrasonic waves will probe the structure, i.e. $\mathbf{D}^c = 0$, and the nonlinear transverse terms are considered negligible, denoted as "…" in the following, we write

$$\begin{aligned} -p^c &= -3K_c v^c + 9\beta_c K_c \tfrac{1}{2}(v^c)^2, \\ \mathbf{T}^c_D &= \underbrace{2\mu\,\mathbf{D}^c}_{\text{Linear}}. \quad \underbrace{\ldots}_{\text{Nonlinear}} \end{aligned} \tag{31}$$

where K_c is the linear elastic bulk modulus associated with the crack.

The definition of the compressional nonlinearity stems from the Taylor expansion of pressure p^c in Eq. (25) with respect to volumetric strain v^c, where the order zero term is zero, the first order term is linear elastic, being proportional to v^c and the second order (nonlinear) term is proportional to $\frac{1}{2}(v^c)^2$. The parameter β_c is defined to capture the volumetric constitutive nonlinearity as a consequence of the clapping nonlinearity associated with the change of volume during closing and opening.

Putting the pressure relation in (31) in the form (25) we have therefore

$$K\{v\} = K_c\left(1 - \frac{3}{2}\beta_c v^c\right) \tag{32}$$

and the linear and nonlinear terms can be identified by equating this with (28) giving

$$K_c = \frac{1}{2}K_0, \tag{33}$$

and

$$\beta_c = \frac{1}{3}\delta^2\mathcal{N}. \tag{34}$$

It remains now to formulate the tensorial nonlinear isotropic response of an inclusion phase, equate this with the crack response above and use this in the context of micro-mechanics.

3.2. Nonlinear Landau coefficients of inclusions and relations to the crack nonlinearity

The constitutive definition of Cauchy stress in an inclusion $\mathbf{T}^{\text{I}}$ is separated into two components in terms of a linear $\mathbf{T}^{\text{I}}_L$ and nonlinear $\mathbf{T}^{\text{I}}_{NL}$ response respectively, as follows,

$$\mathbf{T}^{\text{I}} = \mathbf{T}^{\text{I}}_L + \mathbf{T}^{\text{I}}_{NL}, \tag{35}$$

reducing to $\mathbf{T}^{\text{I}} = \mathbf{T}^{\text{I}}_L$ for linear inclusions.

The nonlinear constitutive response of the crack is assumed to be of the second order form established by Landau et al. [47], valid for a three-dimensional continuum, see e.g. [48,49], which for an isotropic medium is

$$\mathbf{T}^{\text{I}}_{NL}(\mathbf{E}^{\text{I}}) = \hat{\mathcal{A}}_1(\mathbf{E}^{\text{I}})^2 + \hat{\mathcal{B}}_1(\text{tr}((\mathbf{E}^{\text{I}})^2)\mathbf{I}_2 + 2\text{tr}(\mathbf{E}^{\text{I}})\mathbf{E}^{\text{I}}) + \hat{C}_1(\text{tr}\mathbf{E}^{\text{I}})^2\mathbf{I}_2. \tag{36}$$

The penny-crack limit ensures that the macroscopic response is transversely isotropic for aligned cracks. λ and μ are the Lamé constants and $\hat{\mathcal{A}}_1$, $\hat{\mathcal{B}}_1$, $\hat{C}_1$ are the Landau coefficients, where the following approximation has been applied, since the linear constants are negligible

when compared to the nonlinear ones,

$$\begin{aligned}&\hat{\mathcal{A}}_1 + 4\mu_1 \simeq \hat{\mathcal{A}}_1,\\ &\hat{\mathcal{B}}_1 + \lambda_1 - \mu_1 \simeq \hat{\mathcal{B}}_1,\\ &\hat{C}_1 - \lambda_1 \simeq \hat{C}_1.\end{aligned} \tag{37}$$

In order to relate to the nonlinear crack form, combine Eqs. (29)–(31). Furthermore from (33) write $K_1 = K_c = K_0/2$ and recalling that $\mathbf{D}^c = 0$ we have

$$\mathbf{T}^{\mathrm{I}} = -\frac{1}{2}K_0 \mathrm{tr}\mathbf{E}^{\mathrm{I}}\mathbf{I}_2 - \frac{\beta_c K_0}{4}(\mathrm{tr}\mathbf{E}^{\mathrm{I}})^2\mathbf{I}_2. \tag{38}$$

Compared to the general form (36) one establishes that under the present assumptions, the nonlinear properties are

$$\hat{\mathcal{A}}_1 = 0,\ \hat{\mathcal{B}}_1 = 0,\ \hat{C}_1 = -\beta_c\frac{K_0}{4} \tag{39}$$

and therefore

$$\mathbf{T}^{\mathrm{I}}_{NL}(\mathbf{E}^{\mathrm{I}}) = \hat{C}_1(\mathrm{tr}\mathbf{E}^{\mathrm{I}})^2\mathbf{I}_2. \tag{40}$$

With (34) we have

$$\hat{C}_1 = \hat{C}_c = -\frac{\beta_c K_0}{4} = -\frac{\delta^2 \mathcal{N} K_0}{12} \tag{41}$$

or rather with the scaling of δ^2 we may re-write (35) as

$$\mathbf{T}^{\mathrm{I}} = \mathbf{T}^{\mathrm{I}}_L + \delta^2\tilde{\mathbf{T}}^{\mathrm{I}}_{NL}, \tag{42}$$

with

$$\tilde{\mathbf{T}}^{\mathrm{I}}_{NL} = C_1(\mathrm{tr}\mathbf{E}^{\mathrm{I}})^2\mathbf{I}_2. \tag{43}$$

where

$$C_1 = -\frac{\mathcal{N}K_0}{12} \tag{44}$$

which provides the link between the parameter $\mathcal{N}$ associated with the local single crack problem and the effective inclusion that represents the crack.

4. Effective acoustic nonlinearity

Given that we now have a model for the nonlinear behaviour of the cracks and specifically a model for the effective inclusion properties that represent the nonlinear behaviour of an isolated crack, let us use this in order to determine the effective nonlinear behaviour of the cracked material. For conciseness and computational ease we introduce the notation

$$\mathbf{X} = [(\mathbf{I} + \mathbf{H}\mathcal{G}) + \alpha\mathcal{G}]^{-1} \tag{45}$$

together with $\mathbf{Y} = \mathcal{G}\mathbf{X}$ and $\mathbf{Z} = \mathbf{Y}\mathbf{S}\mathbf{D}^0$ which we note both depend on α as well as the effective linear elastic moduli defined in (6) and written in the current notation as $\mathbf{C}^* = \mathbf{C}^0(\mathbf{I} - \alpha\mathbf{Y})$. Referring to (23) and (40)–(44) we can then write

$$\begin{aligned}\mathcal{G}\mathcal{U}\{\bar{\mathbf{E}}\} &= \mathbf{Z}\tilde{\mathbf{T}}^{\mathrm{I}}_{NL}\{\mathbf{Y}\bar{\mathbf{E}}\}\\ &= C_1(\mathrm{tr}(\mathbf{Y}\bar{\mathbf{E}}))^2\mathbf{Z}\colon\mathbf{I}_2.\end{aligned} \tag{46}$$

The total average stress is written

$$\bar{\mathbf{T}} = \mathbf{C}^*\bar{\mathbf{E}} - \alpha C_1\mathbf{C}^0(\mathrm{tr}(\mathbf{Y}\bar{\mathbf{E}}))^2\mathbf{Z}\colon\mathbf{I}_2. \tag{47}$$

Importantly note that the same non-zero components of $\mathcal{G}$ are also non-zero in $\mathbf{X}$, $\mathbf{Y}$ and $\mathbf{Z}$. This simplifies the analysis significantly.

Our investigation of nonlinearity focuses on a compressional stress wave propagating in the x_3 direction, with zero lateral stresses. The strains $\overline{E}_{11} = \overline{E}_{22} \neq \overline{E}_{33}$ and all shear strains are zero. We investigate the propagation of longitudinal, compressional waves in the x_3 direction, i.e. the only non-zero stress is $\overline{T}_{33}$ and the contributions to this stress are therefore from the Z_{33kl} terms. Given that $Y_{11k\ell} = Y_{22k\ell} = 0$, it is straightforward to show that

$$\overline{E}_{22} = \overline{E}_{11} = -\nu_{A*}\overline{E}_{33} \tag{48}$$

where ν_{A*} is known as the (effective) axial Poisson's ratio as determined from the effective linear elastic modulus tensor via

$$\nu_{A*} = \frac{C^*_{1133}}{C^*_{1111} + C^*_{1122}}. \tag{49}$$

The equation for the tensile/compressive longitudinal stress is rather more complicated thanks to the non-zero components of the tensors introduced above. First note that

$$\begin{aligned}\mathrm{tr}(\mathbf{Y}\bar{\mathbf{E}}) &= Y_{3311}\overline{E}_{11} + Y_{3322}\overline{E}_{22} + Y_{3333}\overline{E}_{33}\\ &= (Y_{3333} - 2\nu_{A*}Y_{3311})\overline{E}_{33}\end{aligned} \tag{50}$$

and

$$\begin{aligned}(\mathbf{C}^0\mathbf{Z}\colon\mathbf{I}_2)_{33} &= C^0_{3311}(Z_{1111} + Z_{1122} + Z_{1133}) + C^0_{3333}(2Z_{3311} + Z_{3333})\\ &\simeq C^0_{3333}(2Z_{3311} + Z_{3333}).\end{aligned} \tag{51}$$

Then, eliminating $\bar{\mathbf{E}}_{11}$ via (48) we find

$$\begin{aligned}\overline{T}_{33} &= \mathcal{E}_*\overline{E}_{33} - \beta_*\mathcal{E}_*\overline{E}^2_{33}\\ &= \mathcal{E}_*(1 - \beta_*\overline{E}_{33})\overline{E}_{33}\end{aligned} \tag{52}$$

where β_* defines the effective nonlinear parameter that characterizes the compressional nonlinearity in the x_3 direction and the effective linear elastic Young's modulus is

$$\mathcal{E}_* = (C^*_{3333} - 2C^*_{3311}\nu_{A*}). \tag{53}$$

The effective nonlinear parameter β_* takes the form

$$\beta_* = C_1\frac{\alpha}{\mathcal{E}_*}(Y_{3333} - 2\nu_{A*}Y_{3311})^2C^0_{3333}\left(2Z_{3311} + Z_{3333}\right) \tag{54}$$

where C_1 is the Landau parameter of the inclusion that represents the effective nonlinear response of the crack that was derived in (44).

5. Numerical validation

Let us now turn to a specific example that allows us to determine the effective nonlinearity of the medium in question and in particular to determine the relationship between the effective acoustic nonlinearity β_*, the density of microcracks α and the nonlinearity of the inclusion β_c. Note that the nonlinear parameter β_c depends on $\mathcal{N}$ associated with the crack under tension and the scaling δ^2, which can be quantified experimentally. Contractions and inversions of transversely isotropic tensors within the tensors $\mathbf{X}$, $\mathbf{Y}$ and $\mathbf{Z}$ are computed using Matlab (The MathWorks, Inc., Natick, Massachusetts, United States).

Let us consider a specific model example where a cancellous bone sample is immersed in water and is interrogated by nonlinear ultrasound at a given central frequency f. The incoming pressure p_w in the water at the back of the sample is registered by a needle hydrophone. The water displacement U_w can be obtained as,

$$U_w = \frac{p_w}{\rho_w c_w 2\pi f} \tag{55}$$

where ρ_w and c_w are the density of water and speed of sound, respectively. Considering that the water gap between the specimen and the hydrophone is small (that is, the attenuation in water will be negligible), the displacement of the particles in the specimen is obtained as

$$U_s = \frac{U_w}{T_{sw}} \tag{56}$$

where T_{sw} denotes the transmission coefficient from bone to water, defined as,

$$T_{sw} = \frac{2Z_w}{Z_s + Z_w} \tag{57}$$

Table 1
Elastic parameters of the crack/effective inclusion. Host density and stiffness properties have been taken from typical bone sample values with $E_0 = 14 \times 10^9[Pa]$, $\nu_0 = 0.4$ [50]

Property		Value	
Displacement in water	U_w	13.5281	[nm]
Displacement in sample	U_s	36.8009	[nm]
Frequency	f	666.67	[kHz]
Speed of sound in water	c_w	1500	[m/s]
Speed of sound in sample	c_s	3700	[m/s]
Lamé modulus	λ^1	1.15×10^{11}	[Pa]
Shear modulus	μ^1	2.349×10^9	[Pa]
Density	ρ^1	1×10^3	[kg/m^3]
Scaling parameter	δ	1×10^{-5}	–
Sharpness parameter	$\mathcal{N}$	7.2×10^{14}	–
Nonlinearity of inclusion	β_c	2.4003×10^4	–
Landau coefficient of inclusion	C_1	22×10^{13}	[Pa]

where $Z_i = \rho_i c_i$, $i = w, s$ is the impedance of a material i. The displacement field and associated longitudinal strain in the sample is, as a first approximation, of the form,

$$U(x, t) = U_s \sin(k_s x - \omega t),\ E_{33}(x, t) = U_s k_s \cos(k_s x - \omega t) \tag{58}$$

where $k_s = \omega / c_s$ is the wave number. The maximal strain is obtained when $\cos(k_s x - \omega t) = 1$, that is $v_c = |-\frac{1}{3}E_{33}| = \frac{1}{3}U_s k_s$. Table 1 summarizes the values of the obtained variables U_w, U_s together with relevant parameters that are employed, for a measured pressure $p_w = 85$ [kPa]. Note that water and bone values for densities, velocities, Lamé constants and displacements have been introduced in order to deduce a consistent and realistic validation of the nonlinear parameters. Results obtained in this section are obtained by implementing the theory developed above with the relevant parameters in Table 1. In particular we calculate the effective Young's modulus $\mathcal{E}_*$ from (53) and the effective nonlinear parameter β_* from (54) with the former as a function of the crack density parameter α and the latter as a function of α as well as the crack aspect ratio δ and the Poisson ratio ν_0.

Figs. 3 and 4 illustrate the dependence of $\mathcal{E}_*$ and β_* (respectively) on the crack density parameter α. Plots have been provided for four different host Poisson ratios noting that for bone $\nu_0 \approx 0.4$. What is particularly striking is the variation in properties with α. The percentage change in effective Young's modulus for an α variation over two orders of magnitude is barely noticeable. Given that the effective density of the medium also remains very close to the host medium in this regime the change in compressional wave speed will be extremely small. In contrast the effective compressional nonlinearity parameter β_* changes significantly over the same range of α values. This prediction of β_* falls in the range of values measured for various types of bone [4] and further justifies the use of nonlinear acoustics as a potential diagnostic tool to detect early stage failure in materials.

In Fig. 5 the parameter β_* is plotted as a function of the crack aspect ratio δ. Variation in this parameter is very small in the parameter regime $10^{-12} < \delta < 10^{-2}$. This illustrates that the parameter is fairly stable with respect to crack aspect ratios in realistic aspect ratio parameter ranges.

Finally, Fig. 6 depicts the dependency of the effective nonlinear acoustic parameter on Poisson's ratio, noting that the maximum of β_* is located around $\nu = 0.425$. This maximal value is located in a region ideal for the case of bone where $\nu_0 \approx 0.4$.

6. Discussion

A nonlinear micro-mechanical approach has been proposed that relates the microscopic properties of a distribution of clapping micro-cracks in damaged materials to the macroscopic measurable acoustic nonlinearity. A 1D contact clapping mechanism inside each micro-crack is hypothesized to be responsible for a component of the quadratic nonlinearity. This relationship is formulated by establishing a bilinear clapping constitutive law, which is subsequently approximated by a Taylor expansion, from which the second order constitutive nonlinearity stems. The simplifying assumption to restrict the effect to second order compressional nonlinearity can be questioned in terms of capturing the full nonlinear dynamics of a clapping crack, and would require further extension in future work. However, there are practical reasons for incorporating such second order behaviour, which are related to the generation of second harmonics. These are measurable with ultrasonic equipment and could potentially be employed to inspect structural functionality and damage. It should be clarified that other possible sources of nonlinearity are not treated in this work, such as hysteretic clapping, crack tip plastic zone, partial closure, or atomistic nonlinearities. Their formulations therefore remain open.

The distributed micro-cracks are treated as individual effective penny-shaped inclusions behaving in the manner formulated above with associated effective properties. These nonlinear inclusions are considered as embedded in a uniform host medium and the overall homogenized response is determined via a nonlinear Mori-Tanaka scheme following Giordano's recent work on the extension of Eshelby's result to small -strain nonlinearity. The effective nonlinear response of the crack is defined by its aspect ratio δ, which is interpreted as a

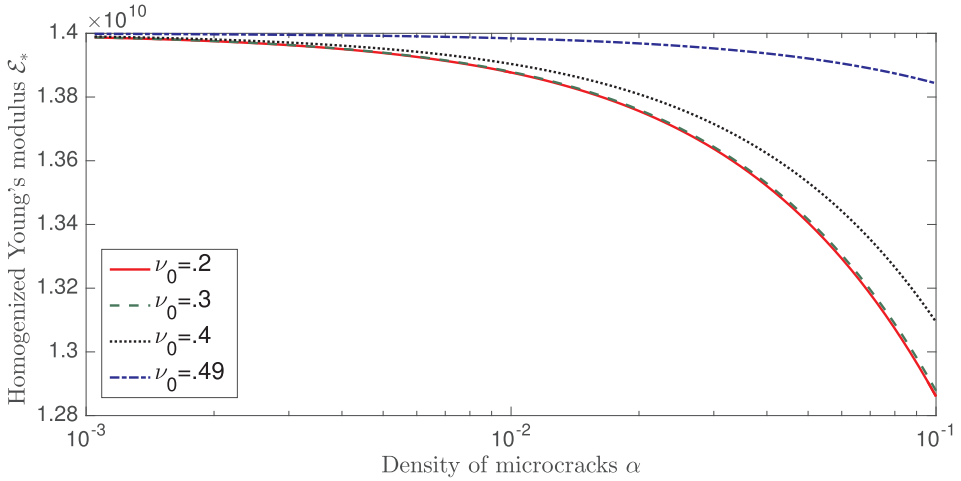

Fig. 3. Illustrating the variation in the linear elastic Young's modulus of the cracked medium $\mathcal{E}_*$ as a function of the crack density parameter α, as defined by (53). The four curves relate to different host medium Poisson ratios. In particular it should be noted that two orders of magnitude change in α leads to a very small change in the predicted $\mathcal{E}_*$.

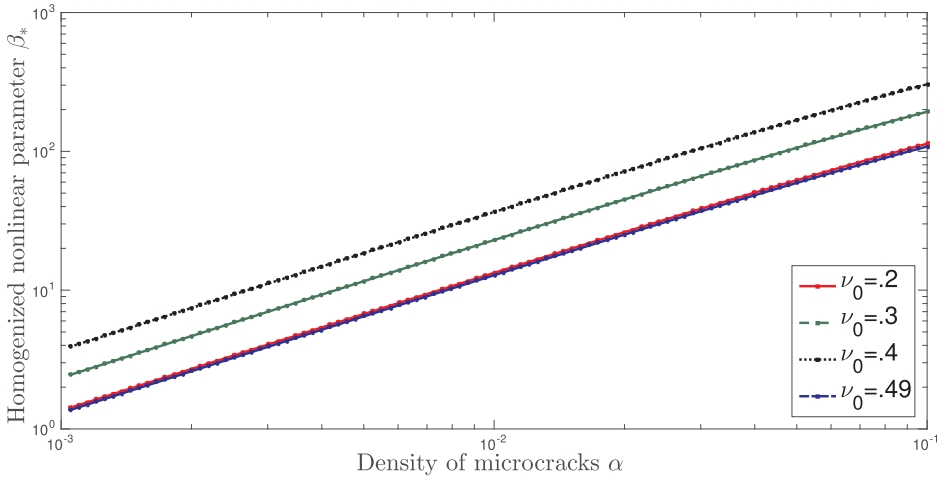

Fig. 4. Illustrating the variation in the effective compressive nonlinearity coefficient of the cracked medium β_* as a function of the crack density parameter α, as defined by (54). The four curves relate to different host medium Poisson ratios. Here it should be noted that two orders of magnitude change in α leads to two orders of magnitude change in β_*. This is in stark contrast to the variation in $\mathcal{E}_*$ with α as noted in Fig. 3.

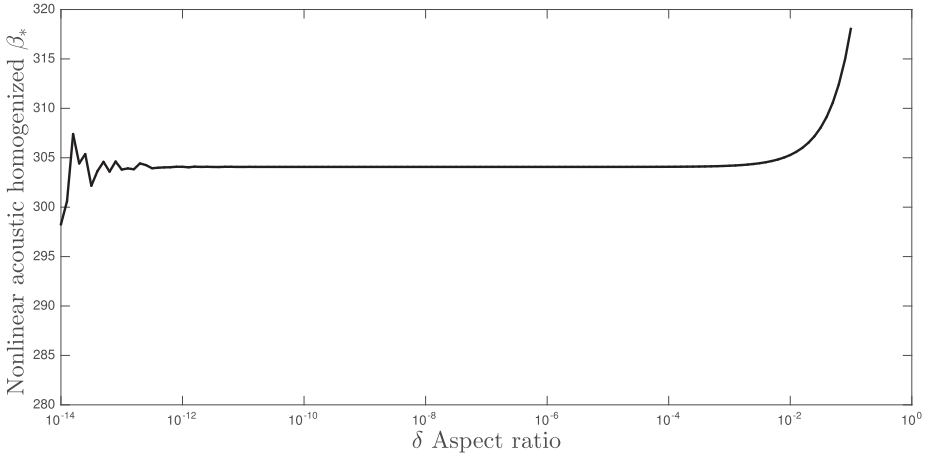

Fig. 5. Illustrating the variation in the effective compressive nonlinearity coefficient of the cracked medium β_* as a function of the crack aspect ratio δ. It is noted that this parameter is relatively insensitive to variations in δ for $10^{-12} < \delta < 10^{-2}$.

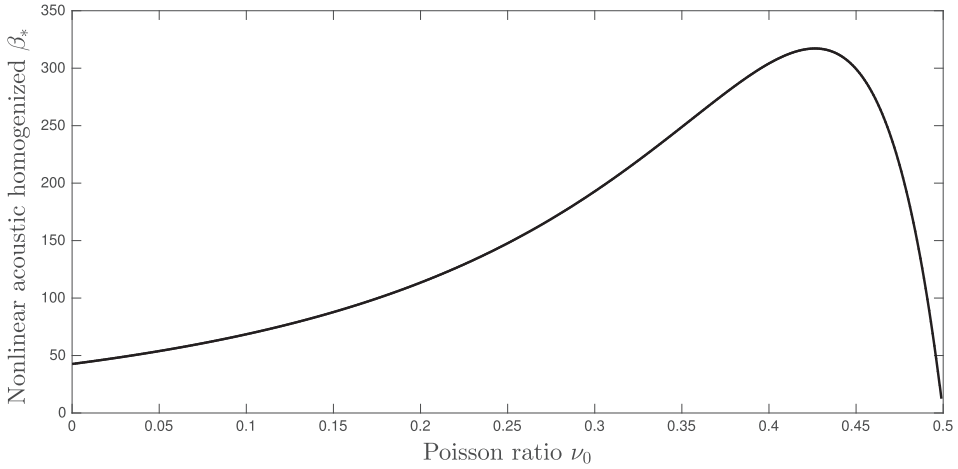

Fig. 6. Illustrating the variation in the effective compressive nonlinearity coefficient of the cracked medium β_* as a function of the host Poisson ratio ν_0. It is noted that for bone $\nu_0 \approx 0.4$, meaning that this is close to where β_* reaches a maximum.

geometric parameter and the nonlinear parameter N, which is interpreted as a material parameter and links to the Landau nonlinearity. Relationships between the measurable acoustic nonlinearity and the Landau-type nonlinearity required by the homogenization scheme are thus proposed. For this purpose, the proposed decomposition of stress and strain tensor into compressional and deviatoric parts plays a key role in redefining several possible acoustic nonlinearities in a convenient way. It should be noted that the model incorporates only a

small number of parameters, which is always beneficial in terms of linkage to experimental data.

The assumption that penny-shaped inclusions are aligned is justified by the fact that fatigue cracks produced by a preferentially-oriented stress appear to be aligned. However, the case of randomly oriented micro-cracks can be developed in future work, by employing the formulation provided in the present paper.

Acknowledgments

The authors acknowledge the Spanish Ministerio de Economía y Competitividad for project DPI2014-51870-R and Junta de Andalucía for projects P11-CTS-8089 and GGI3000IDIB. Melchor is grateful to the University of Manchester for funding via the Engineering and Physical Science Research Council (EPSRC) grant reference EP/I01912X/1. Parnell is grateful to the EPSRC for his research fellowship (EP/L018039/1).

Appendix A. The Eshelby tensor, associated tensors and their strongly oblate limits

TI tensors can be conveniently defined and manipulated by using the Hill basis tensors $\mathcal{H}^{(n)}$ whose components are defined as

$$\mathcal{H}^{(1)}_{ijkl} = \frac{1}{2}\Theta_{ij}\Theta_{kl},\ \ \mathcal{H}^{(2)}_{ijkl} = \Theta_{ij}\delta_{k3}\delta_{l3},\ \ \mathcal{H}^{(3)}_{ijkl} = \Theta_{kl}\delta_{i3}\delta_{j3}, \tag{A.1}$$

$$\mathcal{H}^{(4)}_{ijkl} = \delta_{i3}\delta_{j3}\delta_{k3}\delta_{l3},\ \ \mathcal{H}^{(5)}_{ijkl} = \frac{1}{2}\Big(\Theta_{ik}\Theta_{lj} + \Theta_{il}\Theta_{kj} - \Theta_{ij}\Theta_{kl}\Big) \tag{A.2}$$

$$\mathcal{H}^{(6)}_{ijkl} = \frac{1}{2}\Big(\Theta_{ik}\delta_{l3}\delta_{j3} + \Theta_{il}\delta_{k3}\delta_{j3} + \Theta_{jk}\delta_{l3}\delta_{i3} + \Theta_{jl}\delta_{k3}\delta_{i3}\Big), \tag{A.3}$$

with $\Theta_{ij} = \delta_{ij} - \delta_{i3}\delta_{j3}$ so that the x_1x_2 plane is the plane of isotropy. A fourth order TI tensor $\mathbf{X}$ say, is conveniently written down in terms of the TI basis as

$$\mathbf{X} = \sum_{n=1}^{6} X^n \mathcal{H}^{(n)} \tag{A.4}$$

Further, we find that

$$X^1 = X_{1111} + X_{1122},\quad X^2 = X_{1133},\quad X^3 = X_{3311}, \tag{A.5}$$

$$X^4 = X_{3333},\quad X^5 = X_{1111} - X_{1122},\quad X^6 = 2X_{1313} \tag{A.6}$$

The minor (but not major) symmetries hold and furthermore we note that $X_{1212} = (X_{1111} - X_{1122})/2$.

The inverse $\mathbf{X}^{-1}$ of a transversely isotropic tensor $\mathbf{X}$ is straightforwardly determined as

$$\mathbf{X}^{-1} = \sum_{n=1}^{6} \widehat{X}^n \mathcal{H}^{(n)} \tag{A.7}$$

where

$$\widehat{X}^1 = X_4/\Delta,\quad \widehat{X}^2 = -X_2/\Delta,\quad \widehat{X}^3 = -X_3/\Delta, \tag{A.8}$$

$$\widehat{X}^4 = X_1/\Delta,\quad \widehat{X}^5 = 1/X_5,\quad \widehat{X}^6 = 1/X_6 \tag{A.9}$$

and $\Delta = 2(X_1X_4 - X_2X_3)$.

For a spheroid, the non-zero components of the Eshelby tensor are

$$S_{1111} = \frac{1}{8}\frac{-3\delta^2 + 13L - 4\delta^2 L + 8L\nu_0\delta^2 - 8L\nu_0}{(\delta^2-1)(\nu_0-1)}, \tag{A.10}$$

$$S_{1122} = \frac{-1}{8}\frac{\delta^2 + L - 4\delta^2 L + 8L\nu_0\delta^2 - 8L\nu_0}{(\delta^2-1)(\nu_0-1)}, \tag{A.11}$$

$$S_{1133} = \frac{-1}{2}\frac{2\delta^2 L - \delta^2 + L + 2L\nu_0\delta^2 - 2L\nu_0}{(\delta^2-1)(\nu_0-1)}, \tag{A.12}$$

$$S_{3311} = \frac{1}{2}\frac{-L + \delta^2 - 2\delta^2 L - 2L\nu_0\delta^2 + 2\nu_0 + 4L\nu_0\delta^2 - 4L\nu_0}{(\delta^2-1)(\nu_0-1)}, \tag{A.13}$$

$$S_{3333} = \frac{-2\delta^2 + 1 + 4\delta^2 L - L + \nu_0\delta^2 - \nu_0 - 2L\nu_0\delta^2 + 2L\nu_0}{(\delta^2-1)(\nu_0-1)}, \tag{A.14}$$

$$S_{1313} = -\frac{1}{2}\frac{\delta^2 L + 2L - 1 + L\nu_0\delta^2 - L\nu_0 - \nu_0\delta^2 + \nu_0}{(\delta^2-1)(\nu_0-1)}. \tag{A.15}$$

where

$$L = \begin{cases} \frac{\delta}{4(\delta^2-1)^{3/2}}\left[2\delta(\delta^2-1)^{1/2} + \ln\left(\frac{\delta-(\delta^2-1)^{1/2}}{\delta+(\delta^2-1)^{1/2}}\right)\right], & \delta > 1, \\ \frac{\delta}{4(1-\delta^2)^{3/2}}\left[\pi - 2\delta(1-\delta^2)^{1/2} - 2\arctan\left(\frac{\delta}{(1-\delta^2)^{1/2}}\right)\right], & \delta < 1. \end{cases} \tag{A.16}$$

Here we are interested in limits as $\delta \to 0$. Thus we find that

$$L \sim \frac{\pi}{4}\delta - \delta^2 + O(\delta^3)$$

and therefore the components of the Eshelby tensor in the strongly oblate limit, retaining terms of $O(\delta)$ becomes

$$S_{1111} = \delta\frac{\pi(13-8\nu_0)}{32(\nu_0-1)}, \qquad S_{1122} = \delta\frac{\pi(8\nu_0-1)}{32(\nu_0-1)}, \tag{A.17}$$

$$S_{1133} = \delta\frac{\pi(2\nu_0-1)}{8(\nu_0-1)}, \qquad S_{3311} = \frac{\nu_0}{1-\nu_0} - \delta\frac{\pi(1+4\nu_0)}{8(\nu_0-1)}, \tag{A.18}$$

$$S_{3333} = 1 - \delta\frac{\pi(2\nu_0-1)}{4(\nu_0-1)}, \qquad S_{1313} = \frac{1}{2} - \delta\frac{\pi(\nu_0-2)}{8(\nu_0-1)}. \tag{A.19}$$

so that only $S_{3311} = S_{3322}$, S_{3333} and S_{1313} (with minor symmetries) have non-zero limits as $\delta \to 0$.

Now define $\mathbf{F}^{-1} = \mathbf{I} - \mathbf{S}$ where $\mathbf{I}$ is the fourth order identity tensor whose components are defined by

$$I_{ijkl} = \frac{1}{2}\left(\delta_{ik}\delta_{jl} + \delta_{il}\delta_{jk}\right).$$

Defining $\widehat{\mathcal{F}} = \lim_{\delta\to 0}\mathbf{F}^{-1}$, its only non-zero components are

$$\widehat{\mathcal{F}}_{1111} = 1, \quad \widehat{\mathcal{F}}_{3311} = \widehat{\mathcal{F}}_{3322} = \frac{8\nu_0}{8\nu_0 - 1}. \tag{A.20}$$

Next given that $\mathbf{F} = (\mathbf{I} - \mathbf{S})^{-1}$ we define

$$\mathcal{F} = \lim_{\delta\to 0}\mathbf{F} = O\left(\frac{1}{\delta}\right). \tag{A.21}$$

We also define $\mathbf{G} = \delta\mathbf{F}$ and $\mathcal{G} = \lim_{\delta\to 0}(\delta\mathbf{F})$, the only non-zero components of which are

$$\mathcal{G}_{3311} = \frac{4\nu_0(1-\nu_0))}{\pi(1-2\nu_0)}, \quad \mathcal{G}_{3333} = \frac{4(1-\nu_0)^2}{\pi(1-2\nu_0)}, \quad \mathcal{G}_{1313} = \frac{2(1-\nu_0)}{\pi(2-\nu_0)} \tag{A.22}$$

together with $\mathcal{G}_{3322} = \mathcal{G}_{3311}$ and minor (but not major) symmetries. For finite δ, as should be expected $\mathbf{F}\mathbf{F}^{-1} = \mathbf{I}$ but we note that $\mathcal{F}^{-1}$ does not exist and in particular $\widehat{\mathcal{F}}\mathcal{F} \neq \mathbf{I}$.

Appendix B. Supplementary material

Supplementary data associated with this article can be found, in the online version, at https://doi.org/10.1016/j.ultras.2018.10.009. All results obtained within the paper can be reproduced using formulae provided.

References

[1] J. Krautkrämer, H. Krautkrämer, Ultrasonic Testing of Materials, fourth ed., Springer-Verlag, 1990.
[2] K.-A. Van Den Abeele, P.A. Johnson, A. Sutin, Nonlinear elastic wave spectroscopy (NEWS) techniques to discern material damage, part I: nonlinear wave modulation spectroscopy (NEMS), Res. Nondestr. Eval. 12 (1) (2000) 17–30.
[3] M. Muller, A. Sutin, R. Guyer, M. Talmant, P. Laugier, P.A. Johnson, Nonlinear resonant ultrasound spectroscopy (NRUS) applied to damage assessment in bone, J. Acoust. Soc. Am. 118 (6) (2005) 3946–3952.
[4] G. Renaud, S. Callé, J.-P. Remenieras, M. Defontaine, Non-linear acoustic measurements to assess crack density in trabecular bone, Int. J. Nonlinear Mech. 43 (3) (2008) 194–200.
[5] K.-Y. Jhang, K.-C. Kim, Evaluation of material degradation using nonlinear acoustic effect, Ultrasonics 37 (1) (1999) 39–44.
[6] A.M. Sutin, Nonlinear acoustic nondestructive testing of cracks, J. Acoust. Soc. Am. 99 (4) (1996) 2539–2574.
[7] M.A. Breazeale, D.O. Thompson, Finite-amplitude ultrasonic waves in aluminum, Appl. Phys. Lett. 3 (5) (2004) 77–78.
[8] A.M. Sutin, V.E. Nazarov, Nonlinear acoustic methods of crack diagnostics, Radiophys. Quantum Elec. 38 (3-4) (1995) 109–120.
[9] L.K. Zarembo, V.A. Krasil'nikov, I.E. Shkol'nik, Nonlinear acoustics in a problem of diagnosing the strength of solids, Strength Mater. 21 (11) (1989) 1544–1551.
[10] C.L.E. Bruno, A.S. Gliozzi, M. Scalerandi, P. Antonaci, Analysis of elastic nonlinearity using the scaling subtraction method, Phys. Rev. B 79 (6) (2009) 064108.
[11] T.E. Matikas, Damage characterization and real-time health monitoring of aerospace materials using innovative NDE tools, J. Mater. Eng. Perform. 19 (5) (2010) 751–760.
[12] J.K. Na, W.T. Yost, J.H. Cantrell, Variation of sound velocity in fatigued aluminum 2024-t4 as a function of hydrostatic pressure, Rev. Prog. Quant. Nondest. Evaluation, Springer, 1993, pp. 2075–2082.
[13] J.H. Cantrell, W.T. Yost, Acoustic harmonic generation from fatigue-induced dislocation dipoles, Phil. Mag. A 69 (2) (1994) 315–326.
[14] I.Y. Solodov, Ultrasonics of non-linear contacts: propagation, reflection and NDE-applications, Ultrasonics 36 (1) (1998) 383–390.
[15] D. Donskoy, A. Sutin, A. Ekimov, Nonlinear acoustic interaction on contact interfaces and its use for nondestructive testing, NDT & E Int. 34 (4) (2001) 231–238.
[16] I.Y. Solodov, N. Krohn, G. Busse, Can: an example of nonclassical acoustic nonlinearity in solids, Ultrasonics 40 (1) (2002) 621–625.
[17] A.N. Norris, Finite-amplitude waves in solids, Nonlinear Acoustics 624 (1998).
[18] M. Chekroun, L. Le Marrec, B. Lombard, J. Piraux, Multiple Scattering of Elastic Waves: A Numerical Method for Computing the Effective Wavenumbers, Waves in Random and Complex Media, 2012.
[19] B. Lombard, J. Piraux, C. Gélis, J. Virieux, Free and smooth boundaries in 2-d finite-difference schemes for transient elastic waves, Geophys. J. Int. 172 (1) (2008) 252–261.
[20] B. Lombard, J. Piraux, Numerical modeling of elastic waves across imperfect contacts, SIAM J. Sci. Comput. 28 (1) (2006) 172–205.
[21] S. Nemat-Nasser, M. Hori, Micromechanics: Overall Properties of Heterogeneous Materials, Elsevier, North-Holland, 1999.
[22] S. Torquato, Random Heterogeneous Materials, Springer Verlag, 2001.
[23] G.W. Milton, The Theory of Composites, Cambridge University Press, 2002.
[24] J. Qu, M. Cherkaoui, Fundamentals of Micromechancs of Solids, Wiley, 2006.
[25] J.D. Eshelby, The determination of the elastic field of an ellipsoidal inclusion and and related problems, Proc. R. Soc. A 241 (1957).

[26] W.J. Parnell, The Eshelby, Hill, Moment and Concentration tensors for ellipsoidal inhomogeneities in the newtonian potential problem and linear elastostatics, J. Elast. 125 (2016) 231–294.
[27] W.J. Parnell, C. Calvo-Jurado, On the computation of the hashin-shtrikman bounds for transversely isotropic two-phase linear elastic fibre-reinforced composites, J. Eng. Math. 95 (1) (2015) 295–323.
[28] C. Calvo-Jurado, W.J. Parnell, The influence of two-point statistics on the hashin-shtrikman bounds for three phase composites, J. Comp. Appl. Math. 318 (2017) 354–365.
[29] M. Kachanov, I. Sevostianov, On quantitative characterization of microstructures and effective properties, Int. J. Solids Struct. 42 (2) (2005) 309–336.
[30] S. Giordano, L. Colombo, Effects of the orientational distribution of cracks in solids, Appl. Phys. Lett. 98 (2007) 055503.
[31] R. Spatschek, C. Gugenberger, E.A. Berger, Effective elastic moduli in solids with high density of cracks, Phys. Rev. B 80 (14) (2009) 144106.
[32] S. Giordano, P.L. Palla, L. Colombo, Nonlinear elasticity of composite materials, Eur. Phys. J. B 68 (2009) 89–101.
[33] B.S. Aragh, A.H.N. Barati, H. Hedayati, Eshelby-Mori-Tanaka approach for vibrational behavior of continuously graded carbon nanotube-reinforced cylindrical panels, Compos. Part B: Eng. 43 (4) (2012) 1943–1954.
[34] R. Guyer, P. Johnson, Nonlinear Mesoscopic Elasticity: The Complex Behaviour of Granular Media Including Rocks and Soil, Wiley-VCH, 2009.
[35] S. Delrue, O. -Bou Matar, V. Aleshin, K. Van Den Abeele, Two dimensional modeling of elastic wave propagation in solids containing cracks with rough surfaces and friction - Part I: theoretical background, Ultrasonics 82 (2018) 11–18.
[36] I. Solodov, B. Korshak, E. Ballad, DC, effects, sub-harmonics, stochasticity and “memory” for contact acoustic non-linearity, Ultrasonics 40 (2002) 707–713.
[37] I. Solodov, B. Korshak, Instability, chaos, and memory in acoustic-wave crack interaction, Phys. Rev. Lett. 88 (2002) 014303.
[38] A. Meziane, P. Blanloeuil, C. Bacon, Numerical study of nonlinear interaction between a crack and elastic waves under an oblique incidence, Wave Motion 51 (2014) 425–437.
[39] A. Meziane, A.N. Norris, P.A. Blanloeuil, C. Bacon, Analytical extension of finite element solution for computing the nonlinear far field of ultrasonic waves scattered by a closed crack, Wave Motion 66 (2016) 132–146.
[40] Y. Benveniste, A new approach to the application of Mori-Tanaka theory in composite materials, Mech. Mater. 6 (1987).
[41] F. Lene, D. Leguillon, Homogenized constitutive law for a partially cohesive composite material, Int. J. Solids Struct. 18 (5) (1982) 443–458.
[42] P. De Buhan, A. Taliercio, A homogenization approach to the yield strength of composite materials, Eur. J. Mech. A 10 (2) (1991) 129–154.
[43] D. Fujii, B.C. Chen, N. Kikuchi, Composite material design of two-dimensional structures using the homogenization design method, Int. J. Num. Methods Eng. 50 (9) (2001) 2031–2051.
[44] T.D. Williams, W.J. Parnell, Effective antiplane elastic properties of an orthotropic solid weakened by a periodic distribution of cracks, Q. J. Mech. Appl. Math. 67 (2) (2014) 311–342.
[45] J.B. Walsh, The effects of cracks on the uniaxial elastic compression of rocks, J. Geophys. Res. 70 (1965) 399–411.
[46] C. Pecorari, I. Solodov, Nonclassical nonlinear dynamics of solid surfaces in partial contact for NDE applications, Universality of Nonclassical Nonlinearity, Springer, New York, 2006, pp. 309–326.
[47] L.D. Landau, E.M. Lifshitz, Theory of Elasticity, Pergamon, Oxford, USA, 1986.
[48] S. Catheline, J.-L. Gennisson, M. Fink, Measurement of elastic nonlinearity of soft solid with transient elastography, J. Acoust. Soc. Am. 114 (2003) 3087.
[49] Z. Abiza, M. Destrade, R.W. Ogden, Large acoustoelastic effect, Wave Motion 49 (2) (2012) 364–374.
[50] P. Laugier, G. Haïat, Bone Quantitative Ultrasound vol. 576, Springer, 2011.